Preoperative $^{123}I/^{99m}Tc$-Sestamibi Subtraction SPECT and SPECT/CT in Primary Hyperparathyroidism

Donald R. Neumann[1], Nancy A. Obuchowski[2], and Frank P. DiFilippo[1]

[1]*Department of Nuclear Medicine, Cleveland Clinic Imaging Institute, Cleveland, Ohio; and* [2]*Department of Diagnostic Radiology, Cleveland Clinic Imaging Institute, Cleveland, Ohio*

The trend toward focused surgical parathyroidectomy requires precise preoperative localization of parathyroid lesions in patients with hyperparathyroidism. The purpose of this study was to directly compare the diagnostic accuracy of ^{99m}Tc-sestamibi/^{123}I subtraction SPECT with SPECT/CT for the localization of abnormal parathyroid glands in patients with primary hyperparathyroidism. **Methods:** A total of 61 consecutive surgical patients with primary hyperparathyroidism underwent both $^{123}I/^{99m}Tc$-sestamibi subtraction SPECT and SPECT/CT scans preoperatively, using a hybrid SPECT/CT instrument that combined a dual-detector SPECT camera with a 6-slice multidetector spiral CT scanner. Four hours after being given ^{123}I-sodium iodide orally, each patient received ^{99m}Tc-sestamibi intravenously, followed immediately by a simultaneous, dual-isotope SPECT scan of the neck and upper chest. Then, without moving the patient, we performed a noncontrast-enhanced CT scan of the same body region. Normalization and subtraction of the ^{123}I SPECT images from the ^{99m}Tc SPECT images were performed. The subtraction SPECT and the coregistered fused SPECT/CT studies were interpreted separately, with images scored on a 5-point scale. Surgical and histopathologic findings were used as the standard of comparison. **Results:** Surgery was successful in 57 patients (solitary parathyroid adenoma in 48 patients, double parathyroid adenomas in 6 patients, and 10 hyperplastic parathyroid glands in 3 patients). The sensitivities of SPECT (50/70 = 71%) and SPECT/CT (49/70 = 70%) were similar ($P = 0.779$). The specificity of SPECT/CT (26/27 = 96%) was significantly greater than that of SPECT (13/27 = 48%; $P = 0.006$). The receiver-operating-characteristic area under the curve of SPECT/CT (0.833) was significantly greater than that of SPECT (0.632; $P < 0.001$). **Conclusion:** SPECT/CT is significantly more specific than dual-isotope subtraction SPECT for the preoperative identification of parathyroid lesions in patients with primary hyperparathyroidism.

Key Words: hyperparathyroidism; SPECT; SPECT/CT; hybrid imaging

J Nucl Med 2008; 49:2012–2017
DOI: 10.2967/jnumed.108.054858

Primary hyperparathyroidism is usually a clinical and biochemical diagnosis (*1*). The mainstay of definitive surgical treatment of primary hyperparathyroidism has been routine bilateral neck exploration with attempt to identify 4 parathyroid glands (*2*). Over the last decade, there has been a trend for limited or unilateral surgical neck exploration with resection of the abnormal parathyroid gland with or without identification of an ipsilateral normal parathyroid gland (*3*).

Adjuncts to a successful limited surgical exploration include intraoperative parathyroid hormone (PTH) monitoring, preoperative imaging studies, and, on occasion, intraoperative localization using a handheld γ-probe (*4*). Most experienced endocrine surgeons are proponents for preoperative localization imaging, and most commonly use ^{99m}Tc-sestamibi scans or ultrasonography. Since ^{99m}Tc scintigraphy was introduced by Coakley et al. in 1989 (*5*), it has become the most widely accepted imaging and localizing modality for primary hyperparathyroidism. Adjunctive radiotracers, such as ^{201}Tl-thallous chloride, ^{99m}Tc-pertechnetate, and ^{123}I-sodium iodide, are often added in an attempt to improve ^{99m}Tc-sestamibi scintigraphy by means of image subtraction of the thyroid marker (*6*). The addition of SPECT to ^{99m}Tc-sestamibi scintigraphy has been reported to increase the sensitivity and accuracy of locating abnormal parathyroid glands (*7–9*).

The recent commercial introduction of hybrid SPECT/CT, an instrument that physically couples a SPECT camera with a CT camera in a single integrated unit, offers the potential advantage of better anatomically defining the location of scintigraphic findings that are identified on SPECT images. The incorporation of SPECT with CT, either by offline software fusion (*10*) or by hybrid SPECT/CT techniques (*11,12*), has the potential to further improve preoperative parathyroid imaging. The purpose of this investigation was to directly compare the diagnostic accuracy of ^{99m}Tc-sestamibi/^{123}I subtraction SPECT with SPECT/CT for localization of abnormal parathyroid glands in patients with primary hyperparathyroidism.

Received Jun. 13, 2008; revision accepted Sep. 2, 2008.
For correspondence or reprints contact: Donald R. Neumann, Department of Nuclear Medicine, Cleveland Clinic Imaging Institute, 9500 Euclid Ave., Cleveland, OH 44195.
E-mail: neumand@ccf.org

MATERIALS AND METHODS

A total of 61 consecutive patients with biochemical evidence of primary hyperparathyroidism who were scheduled for parathyroid surgery were studied, including 3 patients with persistent hyperparathyroidism after unsuccessful initial surgery. All patients were referred for preoperative parathyroid ^{99m}Tc-sestamibi SPECT/CT. This study was approved by the Institutional Review Board.

Patients

The study group consisted of 18 men and 43 women with a mean age of 59 y (range, 18–85 y). Before surgery, the median total serum calcium was 11.0 mg/dL (range, 8.8–14.5 mg/dL; reference level, 8.5–10.5 mg/dL), and the median serum PTH was 114 pg/mL (range, 62–768 pg/mL; reference level, 10–60 pg/mL).

Imaging

Four hours after the oral administration of a mean dose of ^{123}I sodium iodide (12,021.3 kBq; range, 10,915–12,765 kBq [324.9 μCi; range, 295–345 μCi]), each patient received a mean dose of ^{99m}Tc-sestamibi intravenously (1,191.4 MBq; range, 1,106.3–1,224.7 MBq [32.2 mCi; range, 29.9–33.1 mCi]). Ten minutes after the sestamibi administration, imaging began. SPECT/CT data were acquired with a Symbia T6 scanner (Siemens Molecular Imaging). The SPECT emission data were collected in dual-energy windows in an attempt to separate the ^{99m}Tc and ^{123}I counts. The ^{99m}Tc window was centered at 140 keV and had 15% width (range, 129.5–150.5 keV). The ^{123}I window was placed with a 4% offset above 159 keV and had 15% width (range, 153.4–177.3 keV). The 4% offset was selected to minimize the spillover of the ^{99m}Tc photopeak into the much less intense ^{123}I photopeak. Before imaging, ^{99m}Tc and off-

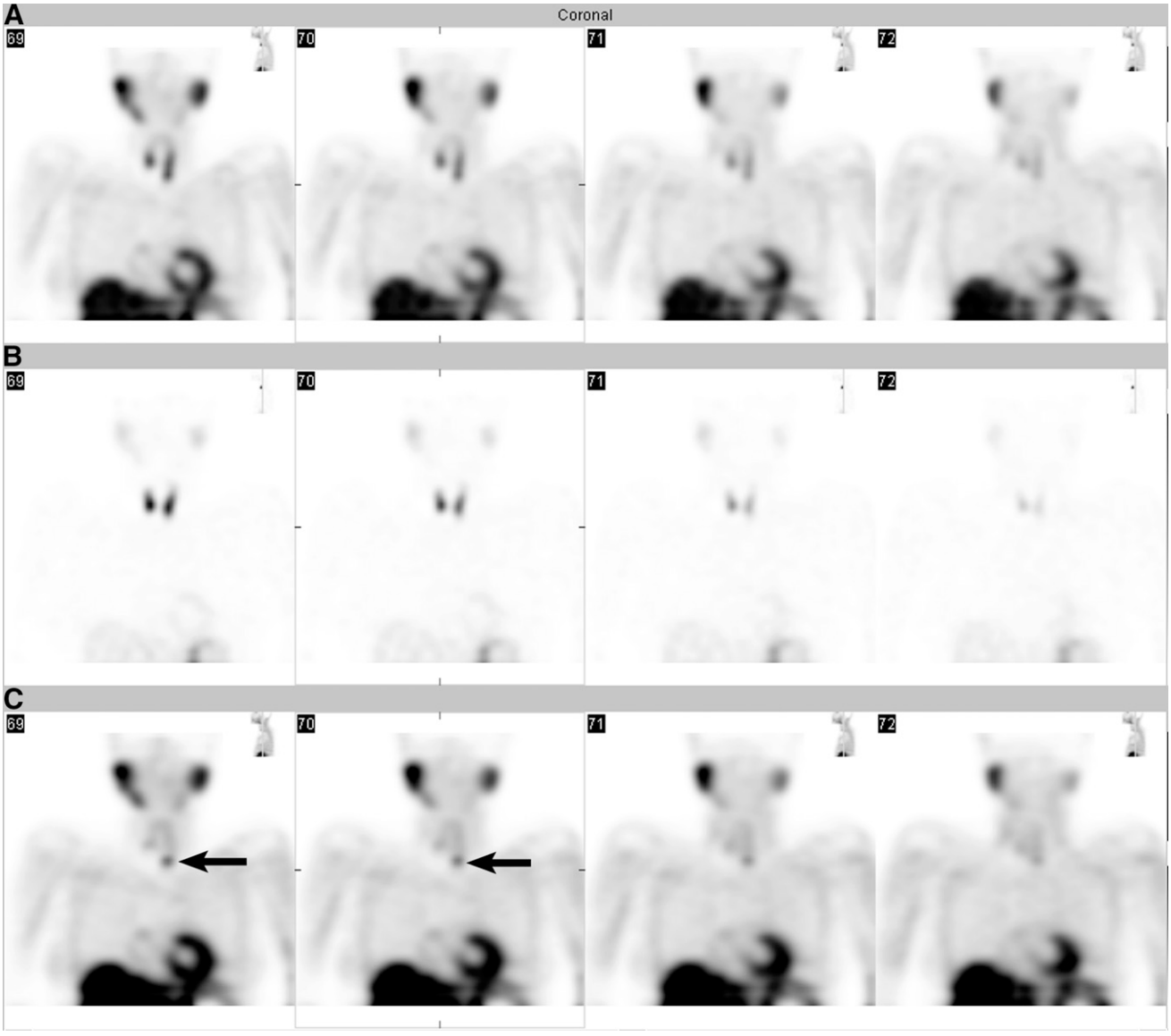

FIGURE 1. Selected series of consecutive coronal dual-isotope SPECT tomograms from scans performed on 61-y-old man with primary hyperparathyroidism. Subtraction of normalized ^{123}I window tomograms (B) from corresponding ^{99m}Tc window tomograms (A) results in subtraction SPECT images (C), which demonstrate small residual focus of activity (arrows) in left lower neck. At surgery, residual focus of activity was found to represent 325-mg parathyroid adenoma.

peak ^{123}I flood images were obtained with the SPECT camera, and all these flood images appeared visually uniform. Emission data were acquired in a step-and-shoot sequence with a contoured noncircular orbit (dual detectors in 180° configuration; low-energy high-resolution collimators; matrix, 128 × 128; pixel size, 4.8 mm; 60 steps per each detector; 3°/step; 25 s/step; total scan time, 25 min). After the SPECT emission scan, the patient remained on the table for the CT portion of the examination; no oral or intravenous contrast agents were administered. After a topogram scout scan (130 kVp, 100 mA, anterior view), a helical CT scan was performed (130 kVp, 6 × 2.0 mm collimation, 0.8-s rotation time, 1.0 pitch). The dose was reduced by tube-current modulation (CARE Dose; Siemens), with the reference exposure set to 80 mAs. Two sets of images were reconstructed. The first set of images, for diagnostic purposes, was reconstructed with a slice thickness of 5 mm at 2.5-mm increments, with a B31s (medium smooth +) filter kernel. The second set of images, used for SPECT attenuation correction, was reconstructed with a slice thickness of 5 mm at 5-mm increments, with a B08s filter kernel. SPECT images were reconstructed on the scanner console workstation using the iterative ordered-subsets algorithm including depth-dependent collimator blur modeling. First, the raw projection data were inspected for patient motion during the scan; if motion was present, the projections were manually shifted to minimize the motion. Next, an initial (non–attenuation-corrected) SPECT reconstruction was performed for each of the 2 acquisition windows. The image-reconstruction settings (FLASH3D software; Easypano) were 4 iterations, 8 subsets, and 8 mm.

Gaussian Postprocessing Filter

The non–attenuation-corrected SPECT and fused SPECT/CT images were displayed to check the accuracy of coregistration. If patient motion was seen between the SPECT and CT images, the CT images were manually shifted to minimize the misregistration. Afterward, the CT images were downsampled to match the SPECT matrix and converted from Hounsfield units into effective attenuation values at 140 keV (^{99m}Tc) and 159 keV (^{123}I). Final SPECT images were then reconstructed with attenuation correction using these CT-derived attenuation maps. The image-reconstruction settings (FLASH3D software) were 4 iterations, 8 subsets, and an 8-mm gaussian postprocessing filter.

Analysis

All studies in this series were interpreted visually in a prospective manner, before surgery, by an experienced nuclear radiologist unaware of the results of any other localization studies. The non–attenuation-corrected SPECT images were evaluated first. ^{123}I SPECT data were first normalized to thyroid tissue on the ^{99m}Tc SPECT data using the image arithmetic tools available on the clinical workstation. An initial normalization factor was determined as the inverse ratio of the maximum voxel value corresponding to thyroid tissue on the ^{123}I SPECT to the value of the corresponding voxel in the ^{99m}Tc SPECT dataset. Each voxel in the ^{123}I SPECT dataset was multiplied by this normalization factor. The normalized ^{123}I SPECT data were then subtracted from the ^{99m}Tc SPECT data to create a subtraction SPECT dataset. In an iterative fashion, the operator was able to adjust this normalization factor until, by visual inspection, subjectively satisfactory subtraction SPECT images were obtained, which were used for interpretation (Fig. 1). A focal site of residual activity on the subtraction SPECT images was defined as a positive finding. Each positive finding was assigned an anatomic location (right or left neck, upper or lower thyroid bed, anterior or posterior superior mediastinum, or other anatomic site) and graded on a 5-point scale of diagnostic confidence (1, definitely negative; 2, probably negative; 3, equivocal; 4, probably positive; and 5, definitely positive for a parathyroid lesion).

At a separate reading session, attenuation-corrected SPECT/CT images were interpreted by the same observer. After normalization

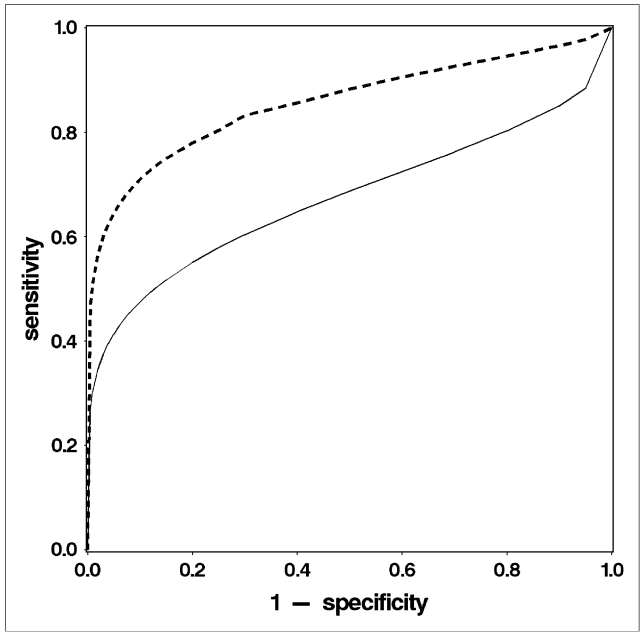

FIGURE 2. ROC curves for subtraction SPECT (solid line) and SPECT/CT (dashed line).

TABLE 1
Accuracies of SPECT and SPECT/CT

Accuracy	SPECT	SPECT/CT
Sensitivity	50/70 = 71% (0.061)	49/70 = 70% (0.062)
Specificity	13/27 = 48% (0.118)	26/27 = 96% (0.038)
ROC area	0.632 (0.067)	0.833 (0.039)

SEs are given in parentheses.

TABLE 2
Effect of Lesion Weight, Calcium, and PTH Levels on Detectability

Parameter	SPECT	SPECT/CT
Mean weight (mg)	TP: 448.0 (402.7) FN: 367.5 (756.2) P = 0.739	TP: 531.1 (588.8) FN: 177.4 (145.0) P = 0.023
Mean calcium (mg/dL)	TP: 11.2 (0.7) FN: 10.9 (1.0) P = 0.467	TP: 11.2 (0.9) FN: 10.9 (0.5) P = 0.097
Mean PTH (pg/mL)	TP: 147.9 (112.1) FN: 112.1 (45.3) P = 0.128	TP: 142.9 (110.4) FN: 125.4 (64.4) P = 0.553

SDs are given in parentheses.

and subtraction of the attenuation-corrected ^{123}I SPECT data from the attenuation-corrected ^{99m}Tc SPECT data, an attenuation-corrected subtraction SPECT dataset was created, which was used for interpretation. Coregistration of the attenuation-corrected subtraction SPECT images with the CT images was performed using fusion software. The operator was able to adjust the window settings, color bars, and mixing ratios of the fused images. A positive finding was defined as focal residual activity on the attenuation-corrected subtraction SPECT image that corresponded to a nonthyroidal soft-tissue lesion on CT images judged to be in an anatomic location consistent with a parathyroid lesion. Each positive finding was assigned this anatomic location and graded on the same 5-point scale as was used for the non–attenuation-corrected SPECT images.

Parathyroid surgery was performed on each patient by experienced endocrine surgeons who were aware of the subtraction SPECT and the SPECT/CT results. The appearance, location, and size of each suspected parathyroid lesion was documented. Histopathologic examination was performed, and weights of all resected surgical specimens were obtained. To estimate sensitivity and specificity for each of the 2 imaging techniques, scores of 1–3 were considered negative and scores of 4–5 were considered positive. The McNemar test, adjusted for the clustered data (i.e., multiple glands per patient) (*13*), was used to compare the sensitivities of subtraction SPECT and SPECT/CT and also to compare their specificities. A significance level of 0.05 was used. Receiver-operating-characteristic (ROC) curves were also constructed for each of the 2 modalities. The areas under the ROC curves of the 2 were compared using methods for clustered paired ROC data (*14*). Generalized linear models, using generalized estimating equations to handle the clustered data (i.e., multiple glands were evaluated in some patients), were fit to assess the association between lesion detectability and gland weight, patient calcium level, and patient PTH level. For each modality, the dependent variable in the model was whether the lesion was a true-positive (TP) or false-negative (FN); the independent variable in the model was lesion weight, calcium level, or PTH level. Because of the small sample size, a multiple-variable model could not be assessed.

RESULTS

There were complete data (SPECT and SPECT/CT results and at least 1 of the following standards of comparison: surgery, histopathology, or CT) on 97 sites from the 61 patients. Parathyroid surgery was successful in 57 patients and provided complete data on 70 of the sites identified by imaging: 48 patients had a single parathyroid adenoma, 6 patients had 2 parathyroid adenomas, 2 patients had 3 hyperplastic parathyroid glands, and 1 patient had 4 hyperplastic parathyroid glands. In the remaining 27 sites identified by imaging, no parathyroid adenoma or hyperplasia was found at surgery. Twelve of these sites exhibited histopathologic correlation: 5 were associated with thyroid adenomas, 3 were associated with multinodular goiter, 2 were associated with Hashimoto thyroiditis, and 2 were associated with thyroid cancer metastases. The other 15 sites were associated with normal anatomic structures on the basis of CT findings (9 normal thyroid, 3 longus colli muscle, and 3 adipose tissue). Table 1 summarizes the accuracy of SPECT and

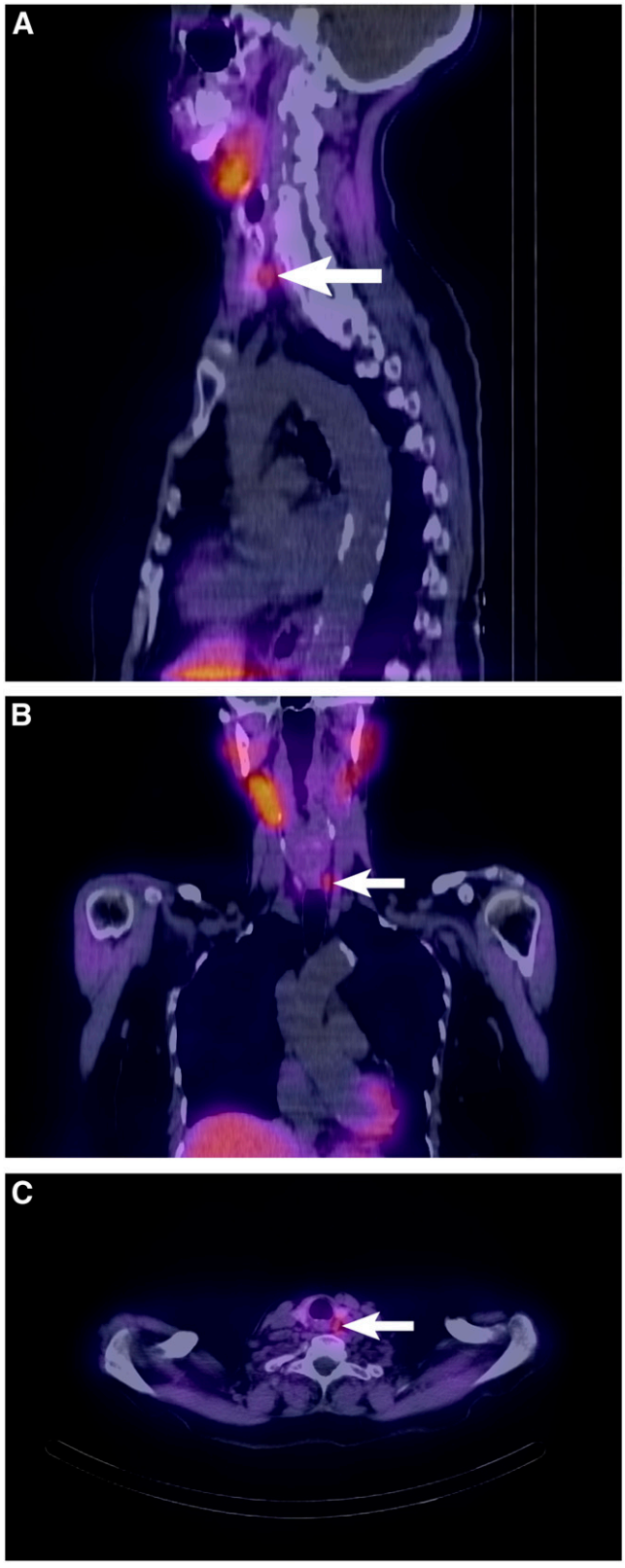

FIGURE 3. Scans performed on 71-y-old woman with primary hyperparathyroidism. Selected fused SPECT/CT sagittal (A), coronal (B), and transverse (C) tomograms demonstrate focus of residual activity associated with soft-tissue nodule (arrow) located posterior to right thyroid lobe. At surgery, residual activity was found to represent 400-mg parathyroid adenoma.

SPECT/CT. The ROC area of SPECT/CT was significantly greater than that of subtraction SPECT ($P < 0.001$) (Fig. 2).

The sensitivity of subtraction SPECT and SPECT/CT were similar ($P = 0.779$). In contrast, the specificity of SPECT/CT was significantly higher than that of subtraction SPECT ($P = 0.006$). Six false-positive subtraction SPECT findings were categorized as true-negatives on SPECT/CT on the basis of their coregistration with normal-appearing thyroid on the CT images. Five false-positive subtraction SPECT findings were categorized by SPECT/CT as true-negatives on the basis of their coregistration with thyroid nodularities on the CT images. Two false-positive subtraction SPECT findings were categorized by SPECT/CT as true-negatives on the basis of their coregistration with longus colli muscle on the CT images.

Table 2 summarizes the results of lesion weight, serum calcium, and serum PTH level analysis, compared with detectability. The calcium and PTH levels were similar in TPs and FNs for both modalities; the weights of the lesions, however, differed between TPs and FNs. The weights for TPs tended to be higher, particularly for SPECT/CT, which reached statistical significance.

DISCUSSION

As the trend toward unilateral or limited surgical neck explorations for the treatment of primary hyperparathyroidism increases, preoperative localization studies have become essential to distinguishing single-gland from multigland disease, differentiating coexistent thyroid pathology, and identifying eutopic, ectopic, and mediastinal parathyroid lesions (*4*). Sestamibi imaging allows the identification of hyperfunctioning parathyroid glands based on their elevated uptake of the radiotracer. However, the degree of anatomic detail provided scintigraphically, using either planar or tomographic techniques, is somewhat limited. Coregistration of sestamibi SPECT with separately acquired CT images has been reported to improve the diagnostic accuracy in detecting hyperfunctioning parathyroid glands (*10,15*). However, with this approach, suboptimal fusing of the 2 imaging modalities due to differences in patient positioning may lead to the incorrect anatomic localization of scintigraphic findings, which, in turn, has the potential to adversely impact the surgical operation and possibly affect patient outcomes. As an alternative approach, hybrid SPECT/CT, which integrates a SPECT camera with a CT scanner in a single instrument, has the advantage of sequentially acquiring SPECT and CT images of the patient in the same position on a single imaging bed. Previous reports have demonstrated the improvement of a SPECT/CT scanner incorporating a low-amperage, single-slice CT scanner over SPECT alone for preoperative parathyroid adenoma localization (*11,16*). Compared with this single-slice system, the use of the multislice spiral CT scanner in the present investigation resulted in much faster CT image acquisitions (<1 min) and thinner CT images of much higher image quality.

Our present study suggests that the SPECT/CT approach is superior to SPECT alone for parathyroid lesion localization, based on further characterization of sestamibi SPECT findings by CT (Fig. 3). In particular, the specificity of SPECT/CT was significantly greater than that of SPECT alone. This

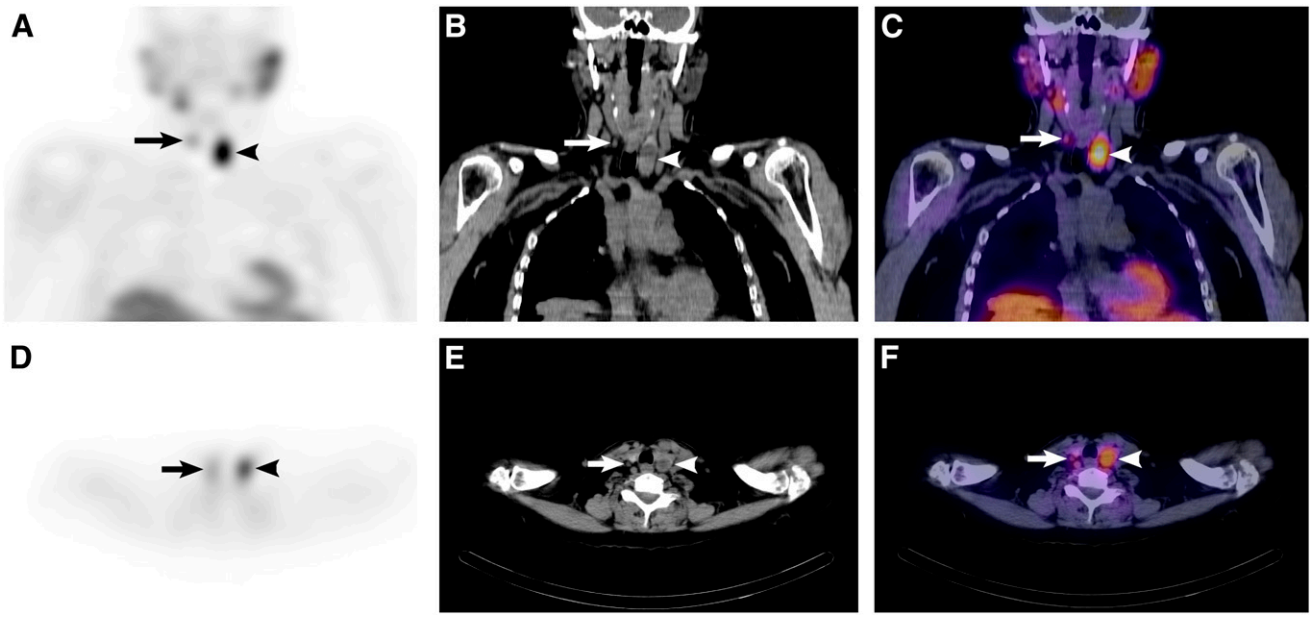

FIGURE 4. Scans performed on 64-y-old woman with primary hyperparathyroidism. Selected coronal (A–C) and transverse (D–F) tomograms of subtraction SPECT (A and D), CT (B and E), and fused SPECT/CT (C and F) demonstrate focus of residual activity associated with small soft-tissue nodule (arrow) located posterior to right thyroid lobe, found at surgery to represent 150-mg parathyroid adenoma. Larger, more intense site of residual activity associated with 3-cm nodule within left thyroid lobe (arrowhead) was found at surgery to represent 5-g well-encapsulated thyroid adenoma.

improved specificity was primarily because of the ability of SPECT/CT to better characterize SPECT findings based on their corresponding CT findings. In some cases, this allowed correct categorization of SPECT findings either as sestamibi-avid nonparathyroid lesions (Fig. 4) or as artifactual, thus reducing the number of false-positive findings.

The estimates of sensitivities for detection of parathyroid lesions reported in this study appear slightly lower than the approximately 78%−100% range of sensitivities reported in other studies (*17*). The sensitivities reported in the present study were calculated for individual parathyroid glands. If these sensitivities were recalculated on a per-patient basis, the sensitivity of subtraction SPECT and SPECT/CT are much higher (88% and 86%, respectively, which are more similar to the previously reported range of sensitivities of ^{99m}Tc-sestamibi scanning for solitary parathyroid adenomas).

Another factor that may have influenced the sensitivities in the present study is the parathyroid lesion sizes in this series. The mean weight of the diseased parathyroid glands in the present study was 425 mg, with more than half of them being less than 300 mg. As is illustrated in Table 2, the sensitivity tends to decrease for smaller parathyroid lesions, reaching statistical significance for SPECT/CT. The mean weight for TPs detected on SPECT/CT was 531.1 mg, compared with 177.4 mg for FNs.

Other factors may have adversely affected the sensitivities reported in the present study. Computer oversubtraction, for example, has the potential to artifactually obscure the visualization of sestamibi-avid parathyroid lesions, although further studies would be required to evaluate this possibility. Although the results of this study are encouraging, they must be considered preliminary because of the relative small size of our patient series. Larger studies of patients with primary hyperparathyroidism, both with and without previous neck surgery, should be examined with this technique to confirm these findings. Future efforts should also be aimed at using some of the other diagnostic capabilities of the multidetector CT scanner, such as various intravenous contrast protocols. Integration of these types of CT studies with sestamibi SPECT may eventually lead to an optimized multimodality imaging approach to preoperative parathyroid localization.

CONCLUSION

The results of our study indicate that SPECT/CT is more accurate than subtraction sestamibi SPECT for the preoperative localization of parathyroid lesions in patients with primary hyperparathyroidism.

REFERENCES

1. Mariani G, Gulec SA, Rubello D, et al. Preoperative localization and radioguided parathyroid surgery. *J Nucl Med.* 2003;44:1443–1458.
2. Wang C. Surgical management of primary hyperparathyroidism. *Curr Probl Surg.* 1985;22:1–50.
3. Chen H, Sokoll LJ, Udelsman R. Outpatient minimally invasive parathyroidectomy: a combination of sestamibi-SPECT localization, cervical block anesthesia, and intraoperative parathyroid hormone assay. *Surgery.* 1999;126: 1016–1021.
4. Sharma J, Mazzaglia P, Milas M, et al. Radionuclide imaging for hyperparathyroidism (HPT): which is the best technetium-99m sestamibi modality? *Surgery.* 2006;140:856–865.
5. Coakley AJ, Kettle AG, Wells CP, et al. 99Tcm sestamibi: a new agent for parathyroid imaging. *Nucl Med Commun.* 1989;10:791–794.
6. Gallowitsch HJ, Mikosch P, Kresnik E, Unterweger O, Lind P. Comparison between 99m-Tc-tetrofosmin/pertechnetate subtraction scintigraphy and 99m-Tc-tetrofosmin SPECT for preoperative localization of parathyroid adenoma in an endemic goiter area. *Invest Radiol.* 2000;35:453–459.
7. Lorberboym M, Minski I, Macadziob S, Nikolov G, Schachter P. Incremental diagnostic value of preoperative 99m-Tc-MIBI SPECT in patients with a parathyroid adenoma. *J Nucl Med.* 2003;44:904–908.
8. Neumann DR, Esselstyn CB Jr, Go RT, Wong CO, Rice TW, Obuchowski NA. Comparison of double-phase ^{99m}Tc-sestamibi with ^{123}I-^{99m}Tc-sestamibi subtraction SPECT in hyperparathyroidism. *AJR.* 1997;169:1671–1674.
9. Billotey C, Sarfati E, Aurengo A, et al. Advantage of SPECT in technetium-99m-sestamibi parathyroid scintigraphy. *J Nucl Med.* 1996;37:1773–1778.
10. Profanter C, Wetscher GJ, Gabriel M, et al. CT-MIBI image fusion: a new preoperative localization technique for primary, recurrent, and persistent hyperparathyroidism. *Surgery.* 2004;135:157–162.
11. Lavely WC, Goetze S, Friedman KP, et al. Comparison of SPECT/CT, SPECT, and planar imaging with single- and dual-phase ^{99m}Tc-sestamibi parathyroid scintigraphy. *J Nucl Med.* 2007;48:1084–1089.
12. Gayed IW, Kim EE, Broussard WF, et al. The value of ^{99m}Tc-sestamibi SPECT/CT over conventional SPECT in the evaluation of parathyroid adenomas or hyperplasia. *J Nucl Med.* 2005;46:248–252.
13. Obuchowski NA. On the comparison of correlated proportions for clustered data. *Stat Med.* 1998;17:1495–1507.
14. Obuchowski NA. Nonparametric analysis of clustered ROC curve data. *Biometrics.* 1997;53:170–180.
15. Ingui CJ, Shah NP, Oates ME. Endocrine neoplasm scintigraphy: added value of fusing SPECT/CT images compared to traditional side-by-side analysis. *Clin Nucl Med.* 2006;31:665–672.
16. Krausz Y, Bettman L, Guralnik L, et al. Technetium-99m-MIBI SPECT/CT in primary hyperparathyroidism. *World J Surg.* 2006;30:76–83.
17. Pattou F, Huglo D, Proye C. Radionuclide scanning in parathyroid diseases. *Br J Surg.* 1998;85:1605–1616.